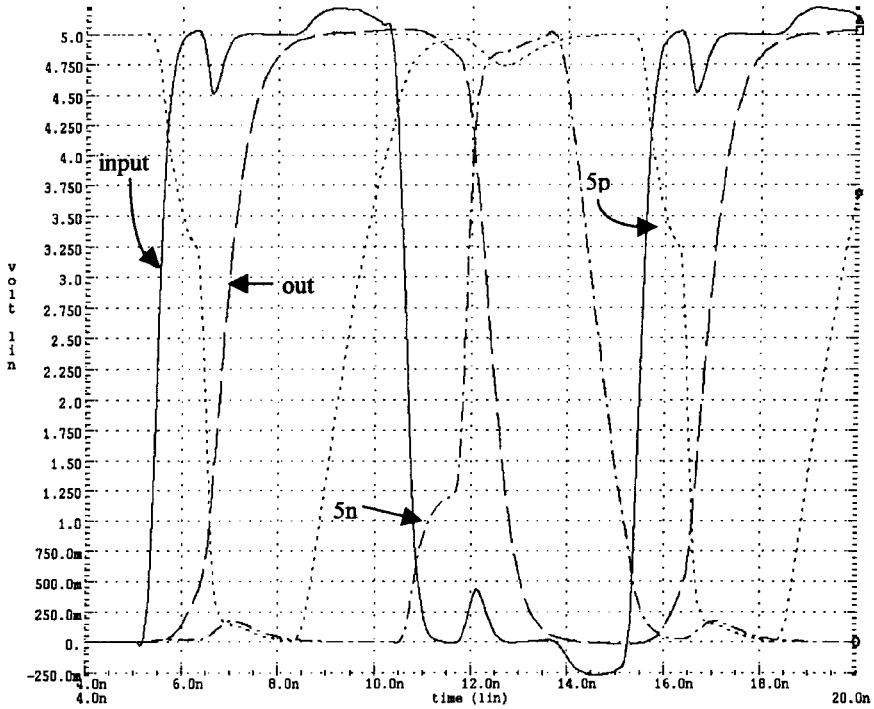

Fig. 4. Simulated waveforms of the CFS CMOS buffer.

delay and lower power dissipation can be achieved by individually sizing the two split-path.

IV. Simulation Results

The power dissipation simulation result of various capacitance loads of the conventional tapper buffer, the FS buffer, and the proposed CFS buffer are shown in Table II. The HSPICE simulation results are based upon the device parameters of 0.6 μm 5 V CMOS process at 100 MHz operating frequency. Table III shows the average propagation delay of the three buffers. Table IV shows the normalized power-delay product simulation results. It is shown that the charge transfer diodes can reduce the propagation delay and power dissipation. It is clear that the proposed CFS CMOS buffer can save over 20% of power-delay product in comparison to conventional tapper buffer.

V. Conclusion

In this brief, the CFS CMOS buffer is proposed and analyzed. The MOS diodes DP and DN are used in the output inverter because the size and the capacitance of the output inverter is large. By using the charge-transfer MOS diodes and feedback control signal, the CFS CMOS buffer can eliminate the short-circuit power dissipation and improve the operation speed. Although the area of the CFS CMOS buffer is increased, simulation results show that over 20% power-delay product savings is possible with the CFS CMOS buffer. Thus it is suitable for low power high speed applications.

References

[1] H. J. Veendrick, "Short-circuit dissipation of static CMOS circuitry and its impact on the design of buffer circuits," *IEEE J. Solid-State Circuits*, vol. SC-19, pp. 468–473, Aug. 1984.

[2] N. Li, F. Haviland, and A. Tuszynski, "CMOS tapered buffer," *IEEE J. Solid-State Circuits*, vol. 25 pp. 1005–1008, Aug. 1990.

[3] K. Y. Khoo and A. N. Willson, Jr., "Lower power CMOS clock buffer," in *IEEE Proc. ISCAS*, 1994, pp. 355–358.

[4] H.-Y. Huang and Y.-H. Chu, "Feedback-controlled split-path CMOS buffer," in *Proc. ISCAS*, 1996, vol. 4, pp. 300–303.

Nonlinear Distortion Model for VCO-PLL FM Transmission Systems

José C. Pedro, Nuno B. Carvalho, and Raquel C. Madureira

***Abstract*—The nonlinear distortion of frequency or phase modulation systems composed by a voltage-controlled oscillator (VCO) modulator and a phase-locked loop (PLL) discriminator is addressed. Volterra series nonlinear transfer functions up to third order, for an LC Colpitts type modulator and a PLL with simultaneous nonlinear phase-detector and VCO, are combined as a cascade of mildly nonlinear systems. This approach gives a fully analytical description of that complex arrangement, which allowed the derivation of theoretical linearization conditions for that FM/PM modem.**

***Index Terms*— Frequency modulation, intermodulation distortion, phase-locked loops, Volterra series.**

I. Introduction

The performance of a general telecommunications physical channel can be evaluated in terms of dynamic range, i.e., the ratio between

Manuscript received July 31, 1997; revised May 30, 1998. This work was supported in part by the Portugese Praxis XXI Program under Project ITCOM. This paper was recommended by Guest Editor A. Rodriguez-Vazquez.

The authors are with the Instituto de Telecomunicações, Universidade de Aveiro, Portugal (e-mail: jcpedro@ieee.org).

Publisher Item Identifier S 1057-7130(99)01770-X.

maximum and minimum detectable signal level for a given output signal-to-noise or intermodulation distortion (IMD) ratio [1]. Beyond the widely known robustness against additive noise, FM or PM are also good modulation methods for IMD immunity: they generate constant envelope modulated signals, which are not capable of driving the system's AM-AM or AM-PM nonlinear characteristics [2]. However, some applications have been reported where the FM modem remains the determinant element on system's IMD performance [3]. Thus, distortion characteristics of analog FM transmission systems are still worth studying.

A voltage-controlled oscillator (VCO) and a phase-locked loop (PLL), represented in the block diagram of Fig. 1, were selected as the FM modulator and frequency discriminator, respectively. Beyond its practical relevance, this type of FM modem was chosen due to the linearity achieved by many VCO's and the threshold extension provided by the PLL [4].

Nonlinear distortion performance of these circuits was already addressed by several authors [5]–[10]. However, from these works, only the analysis of Van Trees [5] enabled real IMD calculations of multitone excitation, since it was done entirely in the frequency domain using Volterra series. Because the harmonic balance method used by Takahashi *et al.* [8]–[10] has to treat the circuit's nonlinearities in the time domain, it suffers from the same problems recognized for any other time-domain simulators, when the input is composed by some incommensurate sinusoids [2]. Another important advantage attributed to Volterra techniques, over other numerical nonlinear analysis algorithms, resides on its closed-form type of solutions, which can be determinant to the extraction of general qualitative conclusions about the system, or even to its possible optimization. It is also recognized, however, that the application of Volterra series to a circuit requires very laborious algebraic calculations, which makes the method useless for predicting nonlinear behavior beyond third order. In the present case, this mild nonlinearity assumption restricts the study to the PLL under tracking operation.

The first aim of this brief is to present a comprehensive study of the nonlinear distortion provided by a VCO-PLL FM modem and to derive linearization conditions for that transmission system.

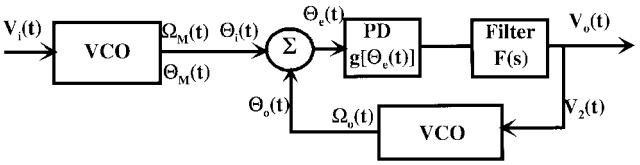

Fig. 1. Block diagram of studied VCO modulator—PLL demodulator FM transmission system (see text).

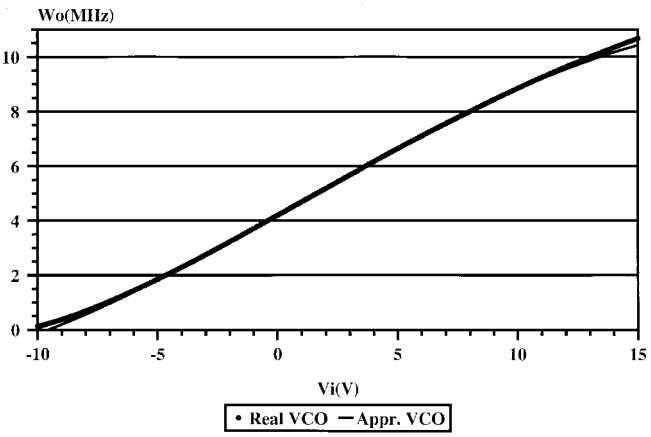

Fig. 2. Comparison between FM modulation characteristics provided by the VCO model and the adopted Taylor series expansion.

II. Volterra Series Model of FM Transmission System

The FM system herein considered assumes a VCO for the modulator (M) and a PLL for the demodulator (D), as described in the block diagram of Fig. 1. Since both of these subsystems are, in general, mildly nonlinear with memory, they should be represented by appropriate Volterra series. Therefore, if their input signal [$V_i(t)$—instantaneous VCO's input voltage, or $\Theta_i(t)$—PLL's instantaneous input phase] is a sum of Q sinusoids, their output [$\Theta_M(t)$—VCO's output phase, or $V_o(t)$—PLL's output voltage] can be expressed as a Volterra series up to third order [2]. There, each of the two subsystems is identified by a set of frequency-domain nonlinear transfer functions, NLTF's, of order n, represented by $H^{(n)}_{M,\,D}(s_1, \cdots, s_n)$.

By applying the probing method [2] to the time-domain nonlinear integro-differential relations of the VCO and the PLL, the derivation of these three $H^{(n)}_{M,\,D}(s_1, \cdots, s_n)$ is straightforward, as can be seen in previously published works of the authors [11], [12].

For the determination of the third-order model of the complete FM transmission system of Fig. 1, we used the classical result of the Volterra series of a cascade of two mild nonlinearities [13]. These generalized chain relations allow the derivation of the whole transmission system's NLTF's, $H^{(n)}_T(s_1, \cdots, s_n)$, as closed-form combinations of the individual $H^{(n)}_M(s_1, \cdots, s_n)$ and $H^{(n)}_D(s_1, \cdots, s_n)$.

In applications where the transmission channel is not transparent, another block [C] could be inserted in Fig. 1, between the VCO and the PLL. If this channel is to be modeled by a dispersive transmission medium, or it includes narrow-band LC band-pass filters at radio-frequency or intermediate-frequency stages of the receiver, then all of its three $H^{(n)}_C(s_1, \cdots, s_n)$ should be evaluated [14]. In any case, the various $H^{(n)}_T(s_1, \cdots, s_n)$ could be determined in much the same way, by recursively applying the generalized chain formulas to the modulator and channel combination, and then to the obtained result and the demodulator.

III. Model Validation

In order to evaluate the validity limits of the proposed model, NLTF's of practical VCO and PLL prototypes are derived and implemented in a computer program. The results thus obtained are then compared to traditional time-domain computer simulations, based on the direct numerical integration of the system's nonlinear equations.

The VCO considered is a transformed Colpitts type sinusoidal LC oscillator. It has a conventional common-base BJT topology where the resonant circuit is composed of two capacitors, C_1 and C_2, in series, connected across an inductor L. In this way, VCO steady-state output frequency can be expressed as

$$\omega_0[v_i(t)] = \left[L\left(C_v[v_i(t)] + C_0 + \frac{C_1C_2}{C_1+C_2}\right)\right]^{-(1/2)} \tag{1}$$

where C_0 is a measured constant varactor parasitic capacitance, and $C_v[v_i(t)]$ is the usual varactor capacitance form [2]. The Taylor series expansion of (1) around the quiescent point $V_{iQ} = 2.8$ V has the following coefficients: $d_{1M} = 3.08$ Mrad/(V·s), $d_{2M} = -14.6$ Krad/(V^2·s), and $d_{3M} = -2.78$ Krad/(V^3·s). A comparison of the frequency modulation characteristics presented by this approximate series and (1) is shown in Fig. 2. A perfect agreement is guaranteed in a wide range of input voltages.

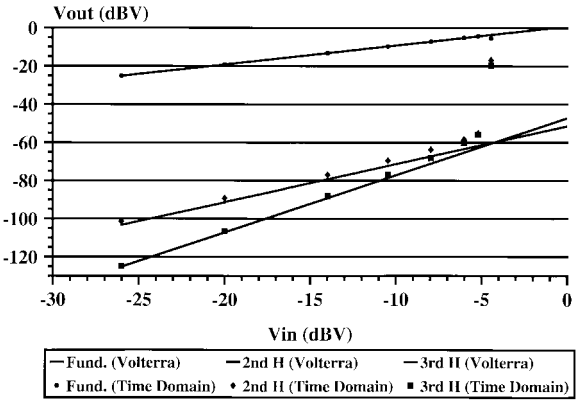

Fig. 3. Comparison of fundamental, second and third harmonic output voltage prediction of FM transmission system using Volterra NLTF's, and time-domain simulations.

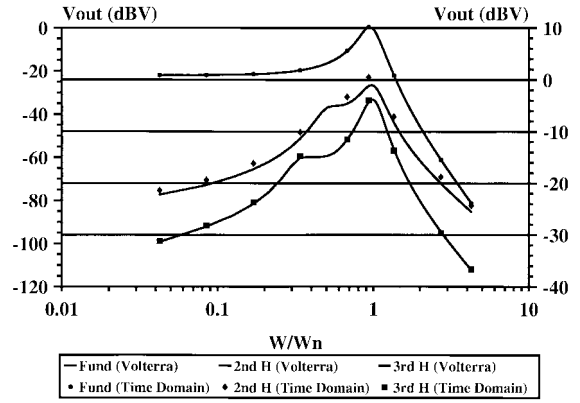

Fig. 4. Prediction of fundamental, second, and third harmonic output voltage versus frequency, obtained with Volterra NLTF's, and time-domain simulations.

The phase detector used in the PLL demodulator is a conventional nonsaturated double balanced RF mixer, which was modeled by an ideal sinusoidal phase-voltage characteristic ($g[\Theta_e(t)]$ in Fig. 1).

For generality purposes, it was assumed that the input central frequency, Ω_i, was slightly different from the demodulator VCO free running frequency, Ω_{0Q}. This imposes a second-degree nonnull term on the Taylor expansion of $g[\cdot]$, although $g[\cdot]$ is, itself, an odd function of $\Theta_e(t)$.

For the selected quiescent point, the Taylor expansion of $g[\cdot]$ gave the following coefficients: $c_1 = 0.78$ V/rad; $c_2 = -0.05$ V/rad^2, and $c_3 = -0.13$ V/rad^3. The PLL discriminator VCO is also a Colpitts, and was modeled using the same procedure above referred for the FM modulator. Its Taylor series coefficients were: $d_{1D} = 2.80$ Mrad/(V·s); $d_{2D} = -20.7$ Krad/(V^2·s), and $d_{3D} = -2.32$ Krad/(V^3·s). Finally, the loop filter was simply chosen as a one-pole RC filter, which has a cutoff frequency of $\omega_c = 250$ Krad/s and leads to a second-order PLL with natural radian frequency, $\omega_n = 739$ Krad/s.

Due to the difficulties of time-domain methods on dealing with noncommensurate frequency excitations, we limited our comparisons to harmonic distortion. Fig. 3 represents simulated results of output amplitude fundamental, second and third harmonic voltage (dBV), versus input drive voltage (dBV), for a fixed input modulating frequency of 5 kHz (4% ω_n). These results were extended to $V_0 = 0.6$ V, which is the point where the PLL was found to loose lock, and therefore may be considered the ultimate limit of the PLL as an FM or PM discriminator. The differences that arise for the higher end of second and third harmonic voltages are due to the PLL, and, within it, to the Taylor series approximation of the sinusoidal PD [11].

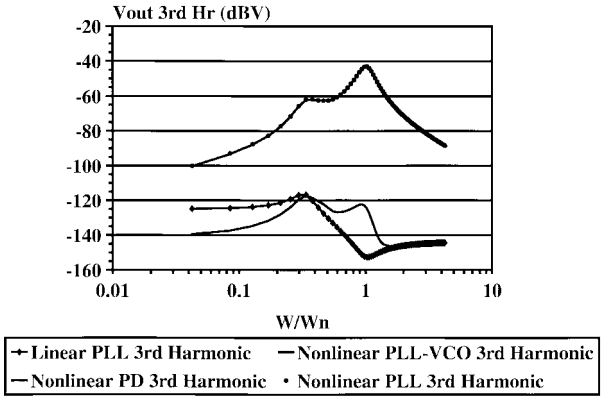

Fig. 5. Separate IMD contributions of FM modulator, discriminator VCO, discriminator PD, and simultaneous discriminator PD and VCO.

Fig. 4 shows first-, second-, and third-order output harmonic distortion versus frequency, for an input voltage amplitude of $V_i = 0.05$ V. The agreement between the two simulated results is now almost perfect in the whole range of modulating frequencies. The slight difference noticed in the second harmonic, near ω_n, can again be attributed to the limited accuracy of the PD Taylor expansion.

IV. Nonlinear Distortion Prediction of an FM Transmission System

In order to evaluate the relative contributions of each of the nonlinear subsystems to the overall distortion, four different conditions were tested. Using the same FM modulator described in the previous section, the nonlinear components of the PLL discriminator were varied to create the following situations reported in Fig. 5: nonlinear VCO and PD, linear VCO and nonlinear PD, nonlinear VCO and linear PD, and linear VCO and PD.

The first conclusion that can be extracted from Fig. 5 is that sinusoidal PD nonlinearity is, by far, the dominant distortion generator of the whole system. Therefore, it is clear that the first step in reducing the IMD of the system is to use a PLL demodulator with a linear PD of triangular or sawtooth phase-voltage transfer characteristic.

Another interesting point that may be observed in Fig. 5 is that the situation of a nonlinear PLL-VCO presents lower third-order harmonic distortion than the full linear PLL, up to 0.3 ω_n. This rather surprising conclusion can be explained by a partial cancellation of the nonlinear distortion components generated at the two modem VCO's.

To determine the exact IMD cancellation conditions, let us derive the complete NLTF's of an FM transmission system, whose PLL discriminator includes a linear PD. Following the procedure referred in Section II, for memoryless modulator (M) and PLL discriminator (D) VCO's, and linear PD, it can be shown that the system's NLTF's up to third order are now

$$H_T^{(1)}(s) = \frac{c_1 d_{1M} F(s)}{s + c_1 d_{1D} F(s)} \tag{2}$$

$$H_T^{(2)}(s_1, s_2) = \frac{d_{2M}}{d_{1M}} H_T^{(1)}(s_1 + s_2) \cdot \left[1 - \frac{d_{2D}}{d_{2M}} H_T^{(1)}(s_1) H_T^{(1)}(s_2)\right] \tag{3}$$

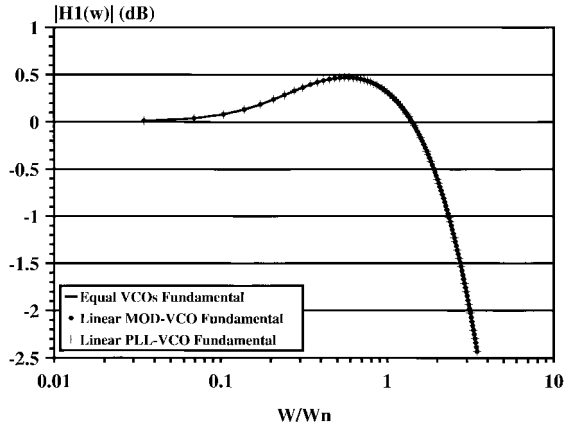

Fig. 6. First-order transfer function for PLL FM discriminator with active loop filter.

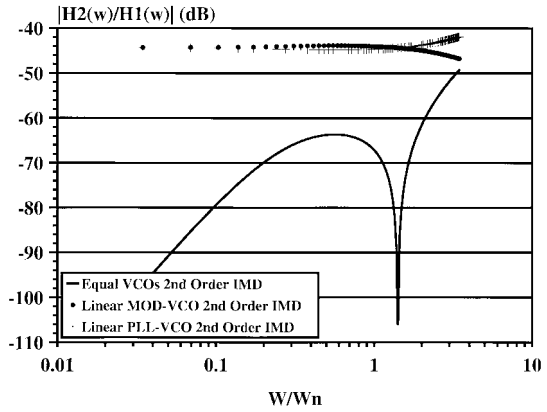

Fig. 7. Second-order distortion for PLL FM discriminator with active loop filter.

$$H_T^{(3)}(s_1,\, s_2,\, s_3) = \frac{d_{3M}}{d_{1M}} H_T^{(1)}(s_1+s_2+s_3) \cdot \left\{ \left[1 - \frac{d_{3D}}{d_{3M}} H_T^{(1)}(s_1) H_T^{(1)}(s_2) H_T^{(1)}(s_3) \right] - \frac{2}{3} \frac{d_{2D}}{d_{3M}} \left[H_T^{(1)}(s_1) H_T^{(2)}(s_2,\, s_3) + H_T^{(1)}(s_2) H_T^{(2)}(s_1,\, s_3) + H_T^{(1)}(s_3) H_T^{(2)}(s_2,\, s_1) \right] \right\}. \quad (4)$$

Expression (3) shows that a system free of second-order distortion can be obtained if the following relation between the two second-degree VCO coefficients and the linear transfer function is verified:

$$\frac{d_{2M}}{d_{2D}} = H_T^{(1)}(s_1) H_T^{(1)}(s_2). \quad (5)$$

Furthermore, if also a similar relation is met for the VCO's third-degree coefficients and the linear transfer function

$$\frac{d_{3M}}{d_{3D}} = H_T^{(1)}(s_1) H_T^{(1)}(s_2) H_T^{(1)}(s_3) \quad (6)$$

an in-band nonlinear distortion free transmission system is found.

Since, in the sinusoidal steady state regime, $H_T^{(1)}(j\omega)$ will change in amplitude and phase, a more or less complex IMD behavior with frequency should be expected for such a linearized FM modem. Because it is dependent on the ratios of d_{2M}/d_{2D}, d_{3M}/d_{3D}, and on $H_T^{(1)}(j\omega)$, we can preview that a careful selection of the modulator and discriminator VCO's associated with a wise design of the PLL loop filter, $F(s)$, would enable a reasonably tight control of the system's nonlinear distortion.

In order to evaluate that possibility in more detail, let us consider the particular situation of identical modulator and discriminator VCO's: $d_{1M} = d_{1D} = d_1$, $d_{2M} = d_{2D} = d_2$, and $d_{3M} = d_{3D} = d_3$.

Noting the form of the first-order system's transfer function (2), it is obvious that, in this case, (5) and (6) are approximately verified when the maximum FM modulation frequency, ω_m, is such that $\omega_m \ll |c_1 \cdot d_1 \cdot F(j\omega_m)|$. For each VCO-PLL combination, ω_m strongly depends on the PLL's loop low-pass filter (LPF).

Because a general approach to this problem was already addressed in [12], the present analysis will be particularized for the more often used active loop filter. Assuming the loop filter's zero at z_1 and the pole at DC, $H_T^{(1)}$ becomes

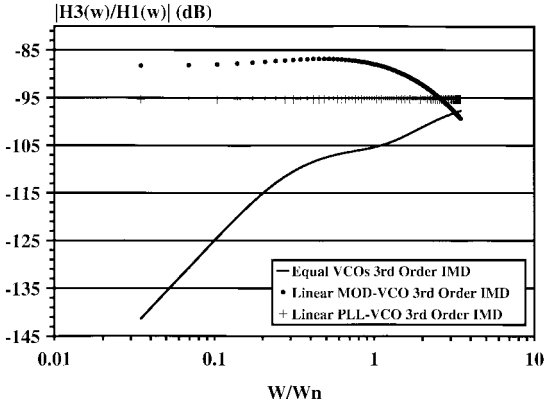

Fig. 8. Third-order distortion for PLL FM discriminator with active loop filter.

$$H_T^{(1)}(s) = \frac{c_1 d_1 A/B(s - z_1)}{s^2 + c_1 d_1 A/B(s - z_1)}. \quad (7)$$

In this case, ω_n can be controlled with z_1. Since this is an active filter, its gain, A/B, can now be used to optimize the system's linear transfer function flatness, within the required bandwidth (see Fig. 6). Moreover, because there is no term in the denominator, other than s^2, that is different from the numerator ones, the system's phase delay is also reduced [12]. The linearization condition is then easily met, which has a direct impact on the system's nonlinear distortion characteristics, as can be observed from Figs. 7 and 8. In fact, the use of this type of LPF provides a useful distortion compensation bandwidth up to about $2.5\omega_n$.

V. Conclusions

A nonlinear Volterra series analytical model up to third order was presented for an FM transmission system composed of a VCO modulator and PLL discriminator. By considering a practical implementation of a PLL with simultaneous nonlinear VCO and phase detector, it was possible to conclude that a sinusoidal PD is, by far, the determinant source of nonlinear distortion. Using a linear PD, a partial cancellation between IMD components generated by the modulator VCO and PLL VCO was detected. This led to the determination of the theoretical optimum IMD condition of equal modulator and demodulator VCO's. That is a rather intuitive IMD cancellation

condition, since it is clear that if the two VCO's are equal, and the PLL is locked with a null frequency error, the developed $V_0(t)$ (which is also the PLL VCO input) must exactly follow the modulator input voltage $V_i(t)$.

As the proposed model predicted different IMD cancellation behavior for distinct PLL linear characteristics, a practical PLL configuration including an active loop filter and triangular or sawtooth PD was studied. For that, useful second- and third-order IMD cancellation margins up to $2.5\omega_n$ were obtained, which proves the practical relevance of this study.

REFERENCES

[1] J. Smith, *Modern Communication Circuits.* New York: McGraw-Hill, 1986.
[2] S. Maas, *Nonlinear Microwave Circuits.* Norwood, MA: Artech House, 1988.
[3] R. Ohmoto and H. Ohtsuka, "Performance of FM double modulation for subcarrier optical transmission," *IEICE Trans. Commun.,* vol. E76-B, no. 9, pp. 1152–1158, Sept. 1993.
[4] D. Schilling and M. Smirlock, "Intermodulation distortion of a phase locked loop demodulator," *IEEE Trans. Commun. Technol.,* vol. COM-15, pp. 222–228, Apr. 1967.
[5] H. Van Trees, "Functional techniques for the analysis of the nonlinear behavior of phase-locked loop," *Proc. IEEE,* vol. 52, pp. 894–911, Aug. 1964.
[6] J. Klapper and J. Frankle, *Phase-Locked and Frequency Feedback Systems.* New York: Academic, 1972.
[7] A. Blanchard, *Phase-Locked Loops—Application to Coherent Receiver Design.* New York: Wiley, 1976.
[8] Y. Takahashi and H. Ohmori, "Harmonic distortion of a PLL FM demodulator for periodic signals," *IEEE Trans. Commun.,* vol. COM-28, pp. 1753–1757, Sept. 1980.
[9] Y. Takahashi and Y. Ishiakawa, "Approximate analysis of harmonic distortion of PLL FM demodulator with time delay," *Trans. IECE,* vol. J65-B, no. 3, pp. 336–337, Mar. 1982.
[10] Y. Takahashi and H. Sakagami, "Calculation of harmonic distortion of PLL FM demodulator with time delay," *IEICE Trans. Commun.,* vol. E78-B, no. 9, Sept. 1995.
[11] N. Carvalho, R. Madureira, and J. Pedro, "Prediction of PLL frequency discriminator nonlinear distortion using the Volterra series approach," in *1996 IEEE Circuits Syst. Int. Symp. Dig.,* vol. 3, Atlanta, May 1996, pp. 229–232.
[12] J. Pedro, N. Carvalho, and R. Madureira, "Nonlinear distortion study of FM transmission systems composed by a VCO-PLL association," in *1997 IEEE Circuits Syst. Int. Symp. Dig.,* vol. 2, Hong Kong, June 1997, pp. 957–960.
[13] Y. L. Kuo, "Frequency-domain analysis of weakly nonlinear networks, Part I," *IEEE Circuits Syst. Soc. Mag.,* pp. 2–8, Aug. 1977.
[14] K. Clarke and D. Hess, *Communication Circuits: Analysis and Design.* Reading, MA: Addison-Wesley, 1971.